Oil Palm-Based Nanocellulose: From Extraction to Applications

Hong Jun Lim, Wai Kit Cheng, Khang Wei Tan, and Lih Jiun Yu

Abstract The palm oil industry is the largest contributor of biomass in Malaysia where vast amount of oil palm biomass waste is generated annually while only a small fraction is being converted into value-added products. The remaining is either burnt or left to decompose at the plantations, which will emit hazardous gases and often resulting in acute air pollution. Much effort has been invested for a more sustainable palm oil circular economy, in which the exploitation of lignocellulosic residues for nanomaterials production can be the golden answer. Nanocellulose may prove to be one of the most auspicious green materials for nanocomposite processing owing to its superb mechanical properties, abundance, renewability and biodegradability. Nanocellulose has garnered increasing attention over the last few decades due to its great potential in diverse applications including food industry, biomedical field, environmental remediation, construction composite materials, corrosion protection and catalysis. This chapter provided a comprehensive review of the recent advancements of oil palm-based nanocellulose from its initial isolation, characterizations to the final applications. Ultimately, the challenges and opportunities for future development associated with the commercialization of nanocellulose-based materials were also thoroughly canvassed.

Keywords Biomass · Nanocellulose · Nanocomposite · Food packaging · Biomedical · Effluent treatment

H. J. Lim · W. K. Cheng · K. W. Tan (✉)
School of Energy and Chemical Engineering, Xiamen University Malaysia, Selangor Darul Ehsan, 43900 Sepang, Malaysia
e-mail: khangwei.tan@xmu.edu.my

L. J. Yu
Faculty of Engineering, Technology and Built Environment, UCSI University, Kuala Lumpur Campus, No. 1, Jalan Menara Gading, UCSI Heights (Taman Connaught), Cheras, 56000 Kuala Lumpur, Malaysia

1   Introduction

Biomass can be defined as organic matters consisting of carbon, oxygen, nitrogen and hydrogen originated from agricultural wastes and residues, forestry, as well as the biodegradable fractions of industrial and municipal wastes. Biomass is widely known for its potentials to supply myriads of different bioenergy such as biogas, briquettes and biofuels that contribute to the reduction of global greenhouse gas emissions. Biomass also plays an indispensable role in the production of renewable chemicals and biomaterial products including bio-fertilizers and bio-composites. Oil palm biomass refers to agricultural by-products originated from the palm oil industry during milling, replanting and pruning activities (Onoja et al., 2019). It can generally be classified into oil palm trunks (OPT), oil palm fronds (OPF), empty fruit bunches (EFB), mesocarp fiber (MF), palm kernel shell (PKS) and palm oil mill effluent (POME). OPT and OPF are typical examples of oil palm biomass produced at the plantation ; while EFB, MF, PKS and POME are generated at the oil palm processing mills (Onoja et al., 2019; Padzil et al., 2020).

   Malaysia is well-endowed with oil palm and is the second largest producer after Indonesia. The palm oil industry is the fourth largest contributor to the Malaysian's Gross National Income that help generates billions of Ringgits (Onoja et al., 2019). Oil palm is the most important and cultivated agricultural crop in Malaysia, with a total of 5.87 million hectares of plantation area in the year 2020 (Parveez et al., 2021). From the year 2017 to 2019, the average amount of oil palm biomass generated in Malaysia was approximately 22.42 million tonnes of EFB, 7.13 million tonnes of PKS and 71.34 million tonnes of POME. As of February 2020, the amount of EFB, PKS and POME generated were around 2.80 million tonnes, 0.89 million tonnes and 8.92 million tonnes, respectively (Rubinsin et al., 2021). This indicated that oil palm biomass is readily available in Malaysia. Howbeit, only a small fraction of the produced biomass is being converted into value-added products, whereas the remaining large portion are left underutilized. Conventionally, oil palm biomass is either burnt or left at the plantations to decompose naturally, therefore contributing to environmental hazards due to the emission of harmful gases. In order to circumvent the issues raised by the improper disposal of oil palm biomass, future researches are salient to convert this abundant and renewable biomass into different value-added products with various prospective applications (Onoja et al., 2019) (Table 1).

1.1   *Lignocellulosic Components of Oil Palm Biomass*

Oil palm biomass is rich in lignocellulosic, except POME. As elucidated in Table 2, the solid oil palm biomass is mainly comprised of cellulose, hemicellulose and lignin in different proportion, depending on the biomass types. These lignocellulosic biomass materials can be regarded as renewable, sustainable and non-toxic (Onoja et al., 2019; Padzil et al., 2020). Cellulose represents one of the most abundant

Table 1 Different types of oil palm biomass (Onoja et al., 2019; Padzil et al., 2020)

Biomass type	Description	Site of production
Oil palm trunk	Tree trunks of the oil palmtree	Plantation
Oil palm frond	Leaves from the oil palmtree	Plantation
Empty fruit bunch	Remains of fruit bunch after the removal of palm fruits	Mill
Mesocarp fibre	Remains after crude palm oilextraction from mesocarp	Mill
Palm kernel shell	Remains after palm kernel oil extraction	Mill
Palm oil mill effluent	Liquid by-product produced from sterilization and other milling process of fresh fruit bunch	Mill

natural polymers on earth with the annual production of 1.5×10^{12} tons and consists of unique hierarchical structures made up from a millimeter-sized transverse section to angstrom-sized anhydroglucose units (Guzman-Puyol et al., 2019; Thomas et al., 2018). Generally, cellulose is made up of linear β-D-glucopyranose units linked together by β-1,4-glycosidic bonds (Mishra et al., 2018; Sinaga et al., 2018). One of the most prominent and functional characteristics of cellulose is its high degree of hydroxylation along the polymer chains in which each of the non-terminal monomer consists of 3 hydroxyl groups at C_2, C_3 and C_6 atoms (Fig. 1a) (Thomas et al.,

Table 2 Lignocellulosic content of different oil palm biomass

Biomasstype	Cellulose (%)	Hemicellulose (%)	Lignin (%)	References
Oil palm empty fruit bunch	34.10	31.90	25.90	Gan et al. (2020)
Oil palm frond	40.03	27.08	20.00	Azani et al. (2020)
Oil palm trunk	34.44	23.94	35.89	Onoja et al. (2019)
Oil palm mesocarp fiber	17.30	17.90	43.50	Campos et al. (2017)
Palm kernel shell	27.70	21.60	44.00	Onoja et al. (2019)
Oil palm leaf	32.49	22.97	26.00	Onoja et al. (2019)

2018; Vilarinho et al., 2018). Consequently, the hydrogen bonding arises between hydroxyl groups and oxygen atoms that are positioned within the same cellulose molecule (intramolecular) and between the adjacent cellulose chains (intermolecular). These intermolecular hydrogen bonding give rise to the fibrillar structures and semi-crystalline packing of cellulose which endow it with attractive physical properties including high strength and flexibility (Thomas et al., 2018). As elucidated in Fig. 1b, hemicellulose is made up of various monosaccharide units (mainly pentose sugars) and it exists as either homopolymer or heteropolymer. Hemicellulose can be hydrolyzed easily since it is highly soluble in alkalis. Conversely, lignin is an aromatic polymer that contains randomly substituted phenylpropane monomeric units such as syringyl, guaiacyl and p-hydroxyphenyl units (Fig. 1c) (Onoja et al., 2019). It plays a pivotal role in providing structural support in plants (Malucelli et al., 2017). Cellulose became a cynosure of all eyes within the research community due to its environmental friendliness and attractive features such as non-toxicity, low density, high biodegradability, biocompatibility, excellent thermal and mechanical properties, renewability and easy modification (Dai et al., 2018; Mohamed et al., 2015). The relatively high amount of cellulose in the oil palm biomass rendered it a very promising feedstock for the extraction of nanocellulose to produce a plethora of technologically advanced materials for various industrial applications.

1.2 Nanocellulose

Nanocellulose is a novel class of biopolymer in nanoscale dimensions that is creating a revolution in bio-based materials in the twenty-first century for myriads of interdisciplinary applications such as packaging, biomedical, pharmaceuticals, membrane, 3D printing, energy devices and flexible electronics (Fang et al., 2019; Yahya et al., 2015). This is because nanocellulose possesses distinctive properties including high reinforcing strength and stiffness which is often times comparable to Kevlar and steel, large surface area, remarkable optical properties, tailored crystallinity and easy surface functionalization. Nanocellulose is also biodegradable and renewable which
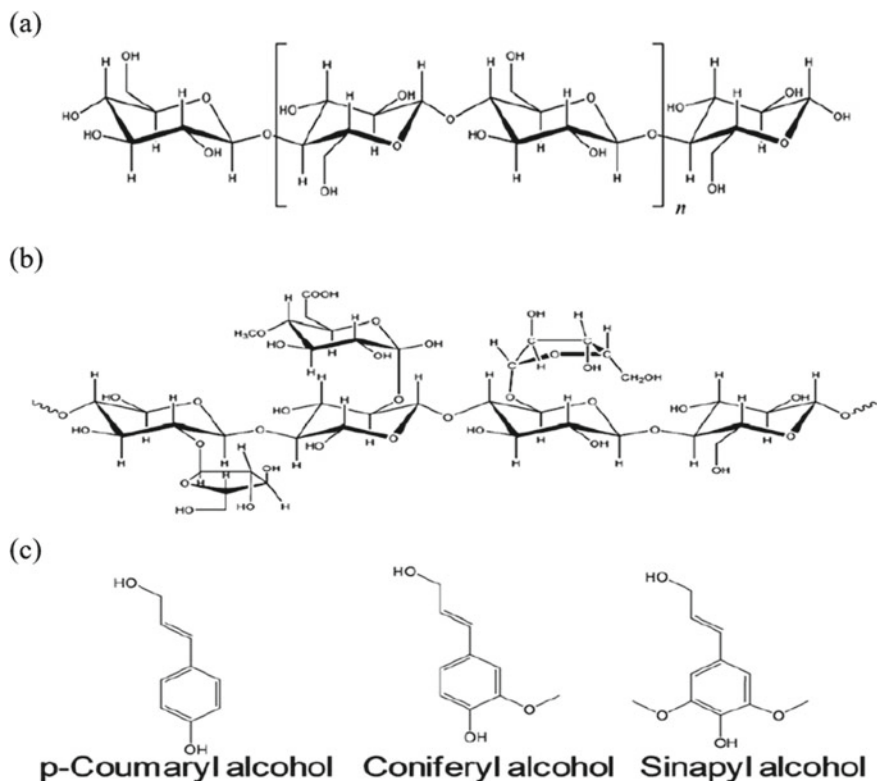
Fig. 1 Chemical structure of **a** cellulose, **b** hemicellulose and **c** lignin (Alonso et al., 2012)

renders it a propitious green alternative for further scrutiny by both the industry and academia (Yahya et al., 2015). Concerning the superior characteristics of nanocellulose, its global market demand stood at USD 87.5 million back in year 2016 and is expected to reach approximately USD 699.6 million in year 2023 with a staggering compound annual growth rate of 33.8%. Some of the key market players of nanocellulose are CelluForce Inc., Fpinnovations, CelluComp, Nippon Paper Group Inc. and Daicel with the current industrial production at tons per day scale. Withal, companies such as Borregaard, Stora Enso and Innventia also manufacture nanocellulose but in a much smaller laboratory scale (Tan et al., 2019).

Conventionally, nanocellulose can be classified into three different categories namely cellulose nanocrystals (CNCs), cellulose nanofibers (CNFs) and bacterial nanocellulose (BNC) according to their morphology and origins. Both CNCs and CNFs are obtained through a top-down approach by disintegrating plant matter through chemical or mechanical treatment. For instance, acid hydrolysis is one of the most common chemical synthesis approaches to produce the highly crystalline or needle-like fragments of CNCs. Contrarily, the mechanical shearing techniques (e.g., high pressure homogenization, grinding and cryocrushing) will disintegrate

Table 3 Classification of nanocellulose

Type of nanocellulose	Synonyms	Typical sources	Average size	Images
Cellulose nanocrystal	Nanocrystalline cellulose, cellulose nanowhiskers and cellulose nanorods	Wood, cotton, hemp, flex, wheat straw, rice straw, ramie, Avicel, tunicin, algae, bacteria etc.	Diameter: 5–70 nm Length: 100–250 nm (from plant); 100 nm-several micrometers (from cellulose of tunicates, algae, bacteria)	
Cellulose nanofiber	Nanofibrils, nanofibrillated cellulose and microfibrillated cellulose	Wood, hemp, flax, sugar beet, potato tuber etc.	Diameter: 5–60 nm Length: several micrometers	
Bacterial nanocellulose	Microbial cellulose, biocellulose	Low molecular weight sugars and alcohols	Diameter: 20–100 nm	

cellulose fibers into their sub-structural nanoscale units, producing longer CNFs that are micrometric in length. Furthermore, BNC is synthesized via the bottom-up approach by utilizing various bacteria cultures to produce the nanomaterial with desired properties (Bharimalla et al., 2017; Thomas et al., 2018). Table 3 shows the summary of the nomenclature used for the three main types of nanocellulose, their origins and average sizes. The next section further elucidates the different nanocellulose extraction methods and their distinct properties.

2   Extraction of Nanocellulose from Oil Palm Biomass

The techniques in which nanocellulose is extracted from oil palm biomass play a pivotal role on the morphology and properties of the resultant materials. This section will examine the main isolation methods used for the extraction of nanocellulose including mechanical treatment, chemical treatment, enzymatic treatment or any combination of these three strategies.

2.1 Pre-treatment

Conventionally, the oil palm biomass obtained from various sources should be milled or triturated to increase the surface area to enhance the subsequent treatments, followed by washing with deionized water to remove any soluble impurities that may be present on the raw materials before further processing. Milling to powder form is necessary to produce uniform particle size and to improve the swelling capacity in water. In addition, raw fibers containing excess impurities might reduce the efficiencies in the following extraction stages (Malucelli et al., 2017). Mazlita's group have performed dewaxing for the OPT fiber via Soxhlet extraction with a mixture of toluene and ethanol since normal water washing may not be efficient in removing the wax and pectin present on the raw fiber's surface. The treated samples are rinsed with deionized water for several times to obtain the wax-free fibers. This step is crucial to increase the accessibility of cellulose toward the subsequent chemical treatments (Mazlita et al., 2016).

2.2 Mechanical Treatment

In general, mechanical treatment refers to a vigorous fibrillation process that isolate CNFs from biomass sources by disintegrating the cellulose along their longitudinal axis. The cellulosic fibers will be broken down into their substructural fibrils with diameter ranging from 10 nm to a few hundred nanometers and length on micrometer scale (Thomas et al., 2018). The common mechanical techniques include high pressure homogenization, micro fluidization and grinding. In high pressure homogenization, the cellulose suspension is pumped into a homogenization machine under high pressure where it will be subjected to shearing and impact forces. These forces will lead to high degree of micro fibrillation of the cellulose slurry. Contrarily, unlike the homogenizer that operates at a constant pressure, the microfluidizer works at a constant shear rate and the cellulose suspension is pumped through a thin chamber with a specific geometry (either Z- or Y-shape). Furthermore, grinding can destroy the structure of plant cell wall by high shear force to produce individual nanofibrils. The cellulose fiber is forced through an ultrafine grinder with two specially grooved disks, one of which is constantly rotating while the other is static. The disk's rotation speed should be maintained at 1500 rpm to avoid clogging in the grinder. The samples must pass through the grinder until a gel is formed. It is noteworthy that the aforementioned mechanical processes should be repeated several times in order to enhance the degree of fibrillation (Ma et al., 2020). Electrospinning, high speed blending, cryocrushing, hammer milling and high intensity ultrasonication are the alternative mechanical treatments reported in the literature (Thomas et al., 2018).

Howbeit, the high energy consumption and production cost are some of the major cumbers to extract nanocellulose from lignocellulosic biomass via mechanical treatment alone. This is because a tremendous amount of energy is required to liberate

the nanocellulose from the natural plant fibers due to the highly ordered hydrogen bond network of cellulose (Thomas et al., 2018). Ergo, numerous pre-treatment techniques have been introduced to reduce the energy consumption up to 98%. One of the archetypal pre-treatment methods is to introduce an electrostatic repulsion between the cellulosic fibers via 2,2,6,6-tetramethylpiperidine-1-oxyl (TEMPO)-mediated oxidation where anionic surface charge (i.e., carboxylate groups) can be incorporated onto the cellulose fibers (Mishra et al., 2018). Unlike any other approaches, TEMPO-mediated oxidation is highly selective and it will only react with the hydroxymethyl group located at C_6 on the glucosyl ring (Tan et al., 2019). Mishra and co-workers epitomized the pros and cons of the different mechanical isolation techniques including micro fluidization, high intensity ultrasonication, electrospinning and steam explosion to obtain the cellulosic nanoparticles (Mishra et al., 2018).

Solikhin and co-workers recently introduced the novel multi-mechanical stages (i.e., dry disk milling, vibrational milling and ultrasonication) for the isolation of lignocellulosic nanofibers (LCNFs) from EFB (Solikhin et al., 2017). The dry disk mill was used to pulverize EFB vascular bundles to produce a finer fraction of approximately 10–20% microsized particles (under 75 μm). The microfibers were then ground using a vibrational pressurized milling to reduce the particle size, destroy silica bodies imparted on the surface of EFB and increase the fibrillation degree of lignocellulosic fibrils. The fiber samples were ultrasonicated to further degrade the polysaccharide linkage via the microjets and shock waves generated during cavitation. This multi-mechanical approach is eco-friendly, inexpensive and easy to implement for large-scale production, indicating its potential to replace the traditional chemical and enzymatic processes.

2.3   Chemo-Mechanical Treatment

Chemical pre-treatments such as alkaline treatment (mercerization) and bleaching (delignification) are conducted to remove non-cellulosic materials such as hemicellulose, lignin and pectin present on the raw fibers (Gan et al., 2020; Malucelli et al., 2017). Alkaline treatment is necessary to partially solubilize the hemicellulose fraction from the oil palm biomass to expose the cellulose structure for further processing. Residual waxes, silica ash and natural fats will also be removed at this stage, while lignin and cellulose are barely affected (Malucelli et al., 2017). Alkaline treatment is usually carried out with 5 wt% NaOH at 80 °C for 1 h followed by washing with deionized water until neutrality (Supian et al., 2020; Thomas et al., 2018). The bleaching process usually takes place after alkaline treatment to remove lignin and residual hemicellulose from the fibers. Two orthodox treatments are well described in the literature archives, namely treatment with 5% sodium chlorite under acidic condition (more effective but hazardous) and 10% hydrogen peroxide under alkaline conditions (Gea et al., 2020; Supian et al., 2020). The bleaching process is often repeated several times to ensure higher level of lignin removal for subsequent hydrolysis treatment. Once cellulose is recovered, acid hydrolysis is employed

to obtain nanocellulose. It is cheaper and more efficient compared to other methods such as enzymatic hydrolysis. During strong acid hydrolysis, the hydronium ions will penetrate the amorphous regions of cellulose chains to cleave the glycosidic bonds and produce highly crystalline cellulose nanoparticles (CNCs). The most commonly used hydrolysing agent is H_2SO_4 where it can react with surface hydroxyl groups of cellulose via esterification process, thus allowing the grafting of anionic sulfate ester groups (Dai et al., 2018; Thomas et al., 2018). The introduction of these negatively charged sulfate groups can promote better dispersion of CNCs in water by electrostatic repulsion (Dai et al., 2018). Other mineral acids including hydrochloric acid, phosphoric acid and nitric acid are also capable of yielding crystalline CNCs but with lower dispersibility in solutions since there is fewer or no charge incorporated on the nanoparticle's surface (Thomas et al., 2018). It is imperative to control the acid hydrolysis process to avoid excessive cleavage of the crystalline regions, which may lower the crystallinity of resultant CNCs and affect their mechanical properties (Malucelli et al., 2017).

After the hydrolysis process, the CNCs suspension is diluted with excess deionized water to quench the reaction. The excess acid is normally removed through a series of centrifugation and washing stages. The precipitate obtained is then subjected to dialysis for removal of non-reactive sulfate groups and soluble sugars. The surplus of sulfate groups may deteriorate the thermal stability of as-synthesized CNCs, although they may also help to prevent the aggregation of nanoparticles. Finally, the CNC suspension is ultrasonicated to ensure the uniform dispersion of nanocellulose followed by freeze drying to produce CNCs in powder form. Drying can reduce the transportation costs and also allows for easier processing in industrial applications. Oven drying and spray drying can also be used as cheaper alternatives besides lyophilization, but these methods may promote the aggregation of CNCs, therefore affecting its final properties (Malucelli et al., 2017).

The neoteric research conducted by Gan's group demonstrated the feasibility of utilizing the novel deep eutectic solvent (DES) as an environmentally friendly alternative for the pre-treatment of EFB to isolate CNCs (Gan et al., 2020). The DES can form hydrogen bonds with lignin and hemicellulose by accepting and donating the protons, thereby improving the solvation ability of EFB fibers. DES can be easily prepared from different mixtures of components at moderate temperature and atmospheric pressure. The conventional alkaline pre-treatment usually involves higher processing costs owing to the significant amount of water required to remove the salts from the treated biomass material. In the study, Gan et al. (2020) first pre-treated the raw EFB with alkaline DES mixture prepared by mixing potassium carbonate and glycerol at a mole ratio of 1:7, followed by bleaching with sodium chlorite solution. The microcellulose obtained was subsequently added into H_2SO_4 solution and centrifuged to obtain a CNC suspension. The suspension was then ultrasonicated to prevent nanocellulose aggregation. The optimum conditions determined for acid hydrolysis were 60 wt% H_2SO_4, hydrolytic temperature of 46.1 °C and reaction time of 58.5 min. The maximum yield of CNCs was 37.1% under the optimum conditions as predicted by the response surface model (Gan et al., 2020). A comprehensive

review concerning the recent development of DES for nanocellulose extraction can be found in the work of Jiang's group (Jiang et al., 2021).

2.4   Enzymatic-Mechanical Treatment

As mentioned briefly in previous sections, the mechanical treatment for nanocellulose extraction requires high energy and high cost, thus it is normally employed as an additional treatment for both chemical and biological methods. Meanwhile, the conventional chemical treatment is highly corrosive and will generate toxic waste. Ergo, biological method such as enzymatic treatment is preferred due to its environmentally friendliness, low energy requirement and production of non-hazardous waste as it allows milder hydrolysis conditions compared to acid hydrolysis (Aditiawati et al., 2018; Thomas et al., 2018). For instance, xylanases are hydrolytic enzymes that can initiate random hydrolysis of β-1,4 non-reducing terminal regions located between the glycosidic linkages of glucose units. Enzymes can also modify or degrade specific components in the cellulosic fibers such as lignin and hemicellulose to yield the desired nanocellulose. Predominantly, the yields of nanocellulose obtained from enzymatic hydrolysis are much lower than those achieved via acid hydrolysis. However, the enzymatic synthesis route can be tuned to fulfil the societal demands on clean chemical processes for the production of state-of-the-art nanomaterials (Thomas et al., 2018).

An elegant example of this approach is the production of CNFs from EFB using the cellulase enzyme from *Trichoderma sp.* (Aditiawati et al., 2018). The non-cellulosic components were first removed from EFB by delignification process via inoculum of *Marasmius* sp. due to its high ligninolytic enzyme activity. Some of the common ligninolytic enzyme produced by *Marasmius* sp. were laccase, mangan peroxidase and lignin peroxidase. The delignified EFB was crushed with cryocrushing method followed by subsequent addition of sodium citrate buffer and crude cellulase ranging from 50 to 200% (v/w). The mixture was incubated for several days before terminating the enzymatic reaction to obtain the desired nanocellulose. Specifically, the addition of 50% (v/w) cellulase enzyme with 2 days incubation time produced almost 100% CNFs with maximum size distribution of 30 nm, indicating the high potential of enzymatic approach for nanocellulose isolation (Aditiawati et al., 2018).

3   Characterization of Nanocellulose from Oil Palm Biomass

Nanocellulose characterization is a crucial subject that had garnered more interest and discussion from experts in tandem with the advancement of nanotechnology and analytical techniques. The primary analytical methods for the characterization of

nanocellulose involve microscopy, spectroscopy as well as thermal and rheological techniques. These types of characterization techniques are employed to determine the morphology of nanocellulose and other features such as crystallinity or mechanical performance (Mishra et al., 2018). It is generally agreed that the morphology and properties of nanocellulose depend on its raw material source and extraction methods. Therefore, it is indispensable to characterize the as-produced nanocellulose to understand its properties before utilizing it for different applications. The following sessions examine the typical characterization techniques employed for nanocellulose extracted from different oil palm biomass.

3.1 Fourier Transform Infrared (FTIR) Analysis

The changes in functional groups of nanocellulose at different treatment stages were analyzed using Fourier transform infrared spectroscopy (FTIR). The spectra were usually recorded in the wavenumber range of 4000–400 cm^{-1} with a resolution of 4 cm^{-1} (Foo et al., 2019; Szlapak Franco et al., 2020). As shown in Table 2, the oil palm biomass is mainly comprised of lignin, hemicellulose and cellulose, or more fundamentally by alkanes, aromatics, esters, ketones and alcohols with different oxygen containing functional groups. In short, the absorption peaks from 3300 to 2900 cm^{-1} were attributed to O–H stretching of hydroxyl groups, while peaks from 2900 to 2800 cm^{-1} can be associated with the aliphatic saturated C–H stretching vibration of cellulose derivatives (Shanmugarajah et al., 2019). Additionally, the peak observed at 1646–1630 cm^{-1} was corresponded to the adsorption of water on cellulose molecules (Gan et al., 2020). The adsorbed water was unable to be removed completely due to the formation of strong hydrogen bonding despite been subjected to the drying process. The peak at 1729 cm^{-1} was accredited to C–O stretching vibration of acetyl and uronic ester groups presented in the ester linkage of carboxylic group of lignin and/or hemicellulose. Furthermore, the peaks located at 1505 and 1592 cm^{-1} were attributed to the aromatic skeletal vibration in lignin (Foo et al., 2019). The typical small peak observed at 1235 cm^{-1} was associated with C–O–C stretching vibration of the aryl group in lignin (Gan et al., 2020). All these characteristic peaks usually disappeared after alkaline treatment and bleaching, indicating the successful removal of hemicellulose and lignin from the oil palm biomass. The peaks in the region of 1420–1430 cm^{-1} were ascribed to the symmetric bending of CH$_2$, whereas the peaks at 1058–1060 cm^{-1} were due to C–O stretching (Foo et al., 2019; Mazlita et al., 2016). Moreover, the presence of β-glycosidic linkages between glucose units of cellulose was illustrated by the peak at 896 cm^{-1} (Szlapak Franco et al., 2020). For the isolation of nanocellulose via sulfuric acid hydrolysis, the presence of negatively charged sulfate ester groups on the surface of CNCs can be identified by the distinct peak located at 1200 cm^{-1} due to S=O vibrations (Foo et al., 2019; Shanmugarajah et al., 2019). The FTIR spectra of cellulose and CNCs displayed similar patterns, suggesting that acid hydrolysis treatment do not significantly alter the chemical

Table 4 FTIR peaks analysis for nanocellulose

Wavenumber (cm^{-1})	Peak assignment	References
3300–2900	O–H stretching of hydroxyl groups	Shanmugarajah et al. (2019)
2900–2800	C–H stretching vibration	Shanmugarajah et al. (2019)
1729	C–O stretching vibration of acetyl and uronic ester groups	Foo et al. (2019)
1646–1630	adsorption of water on cellulose molecules	Gan et al. (2020)
1505	aromatic skeletal vibration in lignin	Foo et al. (2019)
1430–1420	symmetric bending of CH_2	Foo et al. (2019)
1235	C–O–C stretching vibration of the aryl group	Gan et al. (2020)
1200	S=O vibrations	Shanmugarajah et al. (2019)
1060–1058	C–O stretching	Mazlita et al. (2016)
896	β-glycosidic linkages between glucose units	Szlapak Franco et al. (2020)

structure of nanocellulose (Mazlita et al., 2016). Table 4 recapitulates the FTIR absorption peaks for various functional groups in the structure of nanocellulose.

3.2 X-ray Diffraction (XRD) Analysis

The crystallinity of extracted nanocellulose was evaluated by X-ray diffraction (XRD) analysis using the CuKα radiation ($\lambda = 0.154$ nm). The XRD pattern of the samples was typically recorded within the 2θ range from $10°$ to $40°$ (Elias et al., 2017; Gan et al., 2020). The crystallinity index (CrI) of samples was calculated based on the intensity between (002) and (101) lattice diffraction peaks using Segal's method (Eq. 1), where I_{002} represents both the crystalline and amorphous region of cellulose ($2\theta = 22°$) while I_{am} represents only the amorphous phase ($2\theta = 18°$) (Campos et al., 2017; Shanmugarajah et al., 2019).

$$CrI(\%) = \frac{I_{002} - I_{am}}{I_{002}} \times 100\% \tag{1}$$

In the study conducted by Mazlita's group, the XRD patterns of the raw OPT biomass, extracted cellulose and CNCs showed major peaks at $2\theta = 15.6°$, $22.2°$ and $44.4°$, which indicated the presence of cellulose I_β structure (Mazlita et al., 2016). The CrI increased in the order of OPT < cellulose < CNC with the values of 37.37%, 68.35% and 73.17%, respectively. The extracted cellulose displayed higher crystallinity compared to OPT due to the removal of non-cellulosic components (hemicellulose and lignin) during alkaline treatment and bleaching, thus exposing

the cellulose phase for subsequent acid hydrolysis. The highest crystallinity recorded for CNCs can be attributed to the penetration of sulfuric acid molecules into the amorphous structure of cellulose fibers, causing hydrolytic cleavage of glycosidic bonds to release the individual crystallites (Campos et al., 2017; Elias et al., 2017). This lead to the rearrangement of the remaining crystalline regions into a more ordered structure, thus leading to enhance crystallinity of the as-synthesized CNCs (Mazlita et al., 2016). Foo and colleagues also recorded the increased crystallinity of CNCs after acid hydrolysis with CrI of 77.6%, which further substantiates the findings of Mazlita's group (Foo et al., 2019; Mazlita et al., 2016).

Solikhin and co-workers reported pronounced decreased of crystallinity for lignocellulose nanofibers (LCNFs) isolated from EFB via multi-mechanical stages (Solikhin et al., 2017). As compared to the CrI of raw EFB (41.4%), the CrI of LCNFs obtained with 7, 12 and 17 milling times were 24.02, 27.12 and 29.25%, respectively. This phenomenon can be attributed to the high forces involved during vibrational milling process, which damaged the crystalline structure of cellulose. The authors also observed the transformation of cellulose structure from cellulose I to cellulose II after vibrational milling. This might be due to the recrystalline nature of amorphous cellulose in the presence of water from EFB fibers and the heat caused by mechanical friction (Solikhin et al., 2017). Similarly, Franco and associates also observed the decline in CrI (31.5%) for the CNFs extracted from peach palm heart residues via mechanical defibrillation in a colloidal mill (Szlapak Franco et al., 2020). This is because mechanical fibrillation indiscriminately breaks apart both crystalline and amorphous region of cellulose, resulting in lower crystallinity (Campos et al., 2017; Szlapak Franco et al., 2020). Furthermore, the wide XRD peaks observed between 30° and 34° were corresponded to (040) crystallographic plane typical for type I and II cellulose, implying that the combination of chemical pulping and bleaching coupled with mechanical defibrillation transformed the crystalline structure of CNFs from cellulose I to cellulose II. The low crystallinity of cellulose II will contribute to its enhanced dispersibility in water as well as high compatibility with proteins and lipids, thus improving the functionality of the as-fabricated CNF as emulsifying or stabilizing agent in oil/water emulsions (Szlapak Franco et al., 2020).

3.3 Morphological Analysis

The surface morphology of nanocellulose was usually examined using scanning electron microscopy (SEM), field-emission scanning electron microscopy (FESEM) or atomic force microscopy (AFM). Conversely, transmission electron microscopy (TEM) was used to determine the size or dimensions of the extracted nanocellulose. Prior to the characterization, the samples were coated with a thin layer of platinum or gold to reduce the charging effect during analysis (Gea et al., 2020; Supian et al., 2020). The raw oil palm biomass materials typically displayed bundles of individual fibers containing encrusting substances such as lignin, hemicellulose, pectin and waxes. After the pre-treatment process (alkaline treatment and bleaching),

the treated cellulose fibers will exhibit a smoother surface with reduced diameter since most non-cellulosic contents and impurities were removed (Campos et al., 2017). As illustrated in Fig. 2a, CNFs obtained via mechanical fibrillation consist of significant amounts of amorphous regions with long smooth fibrillar structure. This is because the high shear force and intensity produced during nano-grinding causes the cellulose to be broken into smaller sizes, thus yielding nano-dimensioned CNFs (Supian et al., 2020). Solikhin and colleagues observed the agglomerated, irregular and uneven external surface of LCNFs isolated from EFB via multi-mechanical stages with diameters below 100 nm (Solikhin et al., 2017). The aggregation of LCNFs depicted in Fig. 2b can be attributed to the hornification of fibers during oven-heated suspension, as well as strong hydrogen bonding and Van der Waals forces between the nanofibers. The amorphous cementing agents were still deposited on the nanoparticles since no chemical treatment was performed to purify the EFB fibrils. In addition, the high forces of vibrational milling contributed to the destruction of crystalline structure of cellulose, which resulted in highly amorphous and black-colored nanofibers (Solikhin et al., 2017).

On the contrary, CNCs exhibit crystalline rod-like or needle-like shapes with at least one of its dimensions equal to or less than 100 nm (Dai et al., 2018; Thomas et al., 2018). For instance, Gan's group obtained rod-shaped CNCs with
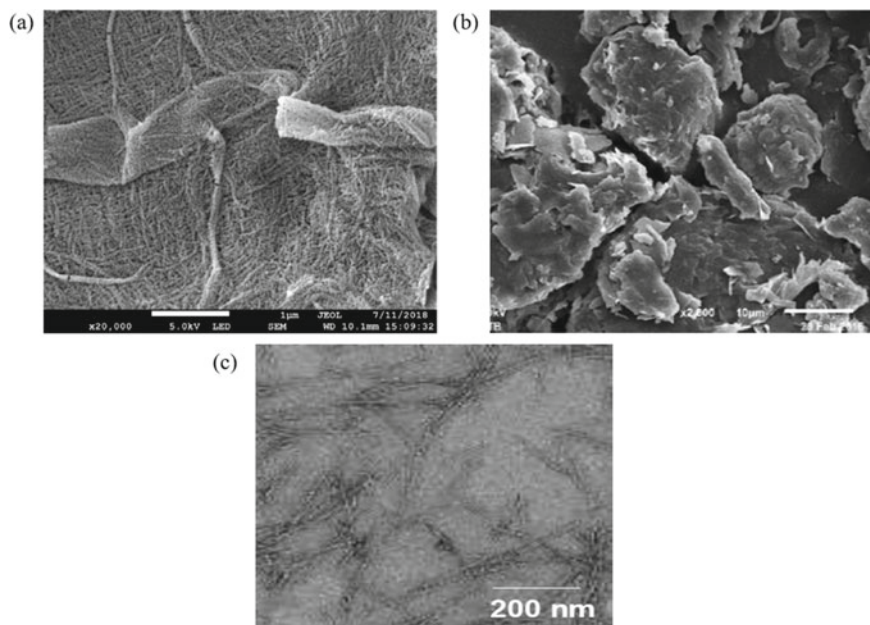
Fig. 2 a FESEM micrographs of CNFs isolated from EFB via nano-grinding with magnification × 20,000, **b** SEM micrographs of LCNFs extracted from EFB by multi-mechanical stages with magnification × 2800 and **c** TEM image of CNCs obtained from EFB (Gan et al., 2020; Solikhin et al., 2017; Supian et al., 2020)

6.78 ± 2.12 nm diameter and 160.06 ± 32.58 nm length from EFB hydrolyzed with 60 wt% H_2SO_4 after DES pre-treatment (Gan et al., 2020). Howbeit, aggregation of CNC was observed in the TEM micrograph of Fig. 2c. This can be accredited to the water evaporation step during sample preparation and the strong hydrogen bonding between CNCs. Interestingly, Campos et. al. (2017) discovered that the mechanical shearing (microfluidizer) would improve the homogenization of nanocellulose morphology in suspension, thereby minimizing the agglomeration of cellulose nanowhiskers without changing the dimensions of the nanoparticles. This novel finding provided additional insights for future researches where the implementation of mechanical shearing after acid hydrolysis could help to reduce the aggregation of nanocellulose, thus maintaining its good dispersion and mechanical performance.

4 Application of Nanocellulose from Oil Palm Biomass

Although the palm oil industry in Malaysia helps to boost the country's economy, it also generates a vast supply of biomass waste. Therefore, managing and processing this biomass waste in a greener approach remains one of the major predicaments by the research communities. One plausible solution is by converting the abundant oil palm waste into new value-added products such as nanocellulose-based composite materials to ensure the sustainable development of the country. Bio-nanocomposite had garnered increased research interest in the past decades due to its biocompatibility, biodegradability and unique functional properties. Bio-nanocomposite can be defined as a combination of a biopolymer and an inorganic moiety with one dimension in nanometer scale (Lamaming et al., 2020). For instance, bio-nanocomposite reinforced with nanocellulose could be used to produce biodegradable food packaging films to reduce the usage of synthetic plastic, whereas its biocompatibility property could be used in tissue engineering or drug carrier. The following sections abridged the current state-of-the-art applications of nanocellulose derived from various oil palm biomass in diverse fields or industries.

4.1 Food Industry

4.1.1 Food Packaging Film

Food insecurity is aggravated as a result of rapid population growth, decreased crop yields due to climate change and higher microbial growth rate at elevated temperature during transportation or storage. Therefore, the food price, trade flow and food access would likely jeopardize the development of a sustainable society in the next few decades (Tan et al., 2019). The ultimate function of food packaging is to ensure the food stability and quality as well as to extend the shelf life of food so that it is safe for human consumption (Azeredo et al., 2017). Nowadays, the usage of

plastic packaging has dominated the food industry by replacing glass and metals (e.g., aluminium or tin) due to its superior flexibility, durability, low cost, ease of processing and broad applicability. In particular, the annual plastics production increased from 1.5 million tons in the 1950s to 359 million tons in 2018. The enormous amounts of plastics produced and its inability to degrade have caused "white pollution" that endangers the Earth's ecological environment. With the temperature rise at both north and south poles, in conjunction with the raging pandemic, protecting the environment and ecosystems has become more acute (Fang et al., 2019; Huang et al., 2020). Withal, plastics are usually derived from existing petroleum reserves, where the scarce resources are dwindling in recent years and cannot be renewed (Sinaga et al., 2018). Ergo, the growth of environmental concerns and public awareness toward the usage of petrochemical-based packaging materials has stimulated interest in biodegradable alternatives originating from replenishable agricultural feedstock (e.g., cellulose, guar gum and starch) or marine food processing industry waste such as chitosan. These types of materials demonstrate huge potential as the environment-friendly substitute for the synthetic plastics (Bhardwaj et al., 2020; Tang et al., 2018). Howbeit, the real-life utilizations of these biopolymers are still a mirage due to their poor mechanical properties, mediocre thermal stability and undesired barrier properties compared to their synthetic counterparts (i.e., plastics). In order to overcome these limitations, the incorporation of nanocellulose represents an efficacious approach to ameliorate the properties of biopolymers, which will expand their application in food packaging sector (El Miri et al., 2015; Tang et al., 2018).

Recently, Lamaming and co-workers prepared a PVA bio-nanocomposite film reinforced with CNCs isolated from OPT using various treatments as an auspicious material for food packaging applications (Lamaming et al., 2020). They reported that all the bio-nanocomposite films displayed higher Young's modulus and tensile strength compared to neat PVA films. The amelioration of mechanical performance can be attributed to the strong hydrogen bond interactions between CNCs and PVA, good compatibility between the fillers and polymer matrix, inherent stiffness of the nanocrystals and homogenous distribution of CNCs within the PVA polymer. The highest tensile strength (88.52 MPa) and Young's modulus (4.86 GPa) were observed for PVA bio-nanocomposite films blended with 5% CNCs with pre-hydrolysis treatment. Interestingly, the CNCs obtained with water pre-hydrolysis treatment had the lowest aspect ratio (L/D) but exhibited the highest tensile strength and Young's modulus (Lamaming et al., 2020). This is counterintuitive because higher aspect ratio of CNC forms more rigid filler network and has better capability to withstand mechanical stress uniformly over the matrix compared to CNC with lower aspect ratio. A plausible explanation might be due to the high zeta potential value of CNCs derived from pre-hydrolysis treatment ($-$ 32.4 mV), thus endowing the good dispersion of nanoparticles in the PVA matrix. Conversely, the elongation at break was found to decrease with higher CNCs loading. This is because the formation of strong hydrogen bonds between the hydroxyl groups on CNC surface and PVA matrix will restrict the mobility of polymer chains, resulting in the decline of overall flexibility of bio-nanocomposite films. Furthermore, the onset degradation temperature and maximum decomposition temperature of all PVA/CNC bio-nanocomposite

films increased by 1–7 °C compared to neat PVA film, suggesting the improvement of thermal stability upon addition of CNCs into PVA matrix (Lamaming et al., 2020).

Solikhin and colleagues also successfully developed PVA/chitosan nanocomposite films incorporated with different concentrations of LCNFs extracted from EFB (Solikhin et al., 2018). The tensile strength of neat PVA/chitosan film increased significantly from 32.19 to 65.65 MPa with only 0.5% LCNFs loadings. The enhancement of mechanical strength at low concentration of nanofillers can be ascribed to the homogeneous and good dispersion of LCNFs in PVA/chitosan matrix. Withal, the high level of compatibility and strong hydrogen bond interactions between LCNFs and PVA/chitosan might also contribute to the improved tensile strength of nanocomposite films, which is consistent with the findings of Lamaming's group (Lamaming et al., 2020; Solikhin et al., 2018). Nevertheless, the tensile strength decreased at higher LCNFs concentration (1, 2.5, 5, 7.5 and 10%) due to the formation of aggregated nanoparticles (Solikhin et al., 2018). A similar observation was also reported by Salehudin and associates where the starch-based biofilm reinforced with 10% CNFs derived from EFB displayed the tensile strength value of 2.90 MPa, which was lower compared to neat starch film (3.66 MPa) (Salehudin et al., 2014). This might be attributed to the agglomeration of nanoparticles at high concentrations that can act as stress concentration points, thereby deteriorating the mechanical performance of the nanocomposite films (Fig. 3a). Moreover, Solikhin and co-workers discovered that the addition of LCNFs induced lower transmittance at 300 nm compared to neat PVA/chitosan film, which is favorable for food packaging materials since it prevents photodegradation reaction between the packaged food and ultraviolet light (Solikhin et al., 2018). As depicted in Fig. 3b, the transparency of PVA/chitosan film reduced with the incorporation of nanocellulose and the effect was more conspicuous at higher concentration of LCNFs. This can be due to the aggregation and low dispersibility of LCNFs in the film matrix. Surprisingly, the as-synthesized PVA/chitosan nanocomposite films did not exhibit anti-bacteria and anti-fungal properties against gram-negative *Escherichia coli*, gram-positive *Staphylococcus aureus*, *Candida albicans* yeast and *Ganoderma* sp. fungi (Solikhin et al., 2018). This is counterintuitive because chitosan is known for its antimicrobial and antioxidant activities (Adel et al., 2019). The reasons postulated by the authors were: (1) water is needed to activate the chitosan as antimicrobial agent since the dried samples used could not release the energy stored inside the chemical bonds to initiate microbicidal reactions; (2) there was no interaction occurred between the cationic chitosan structure with the negatively charged cell membrane of microbes owing to the formation of intermolecular hydrogen bonds between amine groups of chitosan and hydroxyl groups of PVA and LCNFs (Solikhin et al., 2018).

4.1.2 Food Emulsion

Emulsions represent a system of two or more immiscible phases where one is dispersed as droplets in the other(s). The stability of emulsions depends heavily
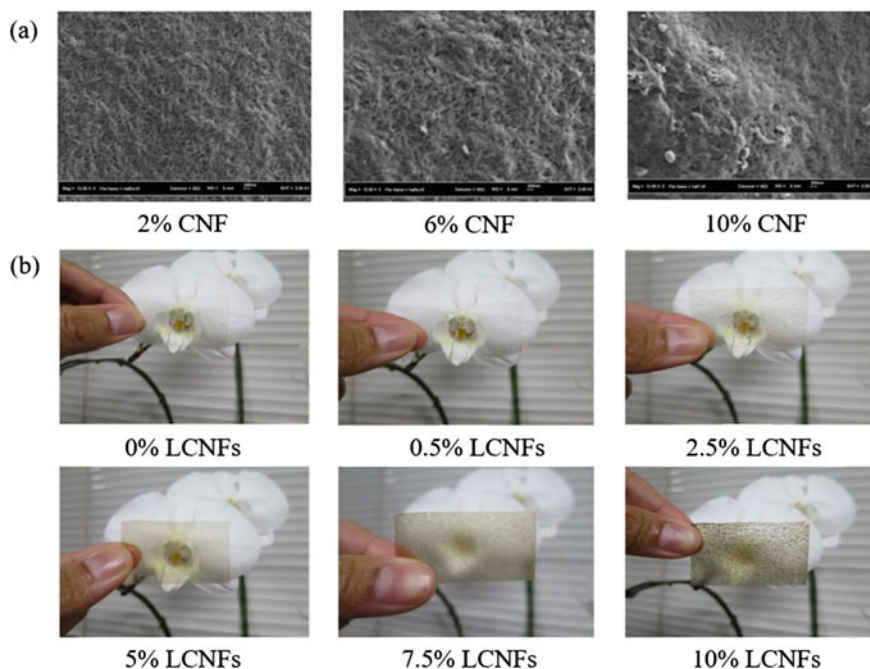
Fig. 3 **a** FESEM images of starch biofilm with different CNF concentration (×12,000 magnification and 200 nm scale) and **b** visual image of PVA/chitosan composite films at different LCNFs concentration (Salehudin et al., 2014; Solikhin et al., 2018)

on their formulation, emulsification techniques and emulsifier agent used that facilitate the interaction between different phases and deliver specific functional properties (Szlapak Franco et al., 2020). Emulsions can be used in plethora of industrial systems, especially in food, cosmetic and pharmaceutical products. Nonetheless, such systems are not thermodynamically stable and will often lead to phase separation to reduce the interfacial tension between the two phases. Ergo, amphiphilic molecules known as surfactants are added to stabilize these systems by reducing the interfacial energy to prevent the phase separation (Perrin et al., 2020). A wide variety of synthetic and natural additives that proportionate stability and emulsification can be legally used in food, including polysaccharides, proteins, phospholipids and small-molecule surfactants. The current consumer conscience about the relationship between personal health and food had stimulated the increased demand for functional and organic foods that are free of chemicals or harmful additives, indicating that the application of new natural emulsifiers is essential to fulfil the social requirements without compromising the sensorial attributes. These natural emulsifiers must display good emulsifying and stabilizing properties to maintain the emulsion characteristics and stability even under the extreme conditions applied during the production, storage and transporting stages (Szlapak Franco et al., 2020). Nanocellulose can be utilized as stabilizer for oil in water emulsions due to its amphiphilic nature and high aspect

ratio. This type of particle stabilized emulsions shielded by a layer of solid particles are known as Pickering emulsions, where the formation of mechanical barrier stabilizes the emulsions against changes of temperature, pH, salt concentration and ionic strength (Perrin et al., 2020; Szlapak Franco et al., 2020).

In the neoteric research conducted by Franco's group, the authors proposed combining the functionality of CNF and health benefits of avocado oil to deliver a food emulsion that could be used without compromising the consumer blood fat levels and also to aid weight loss (Szlapak Franco et al., 2020). This is due to the potential of CNF as food additive or supplement that can reduce the adsorption of fat and limit the diffusion of glucose. They observed that the avocado oil/water emulsions prepared with CNF exhibited a negligent creaming index, indicating the capability of nanoparticles to maintain the emulsion format and their aggregation between the oil droplets even at a wide pH range. This phenomenon can be elucidated by the Pickering mechanism where the formation of CNF fibrillar network dispersed on the water and oil interface can prevent the coalescence of the emulsion droplets and mechanically stabilizing the system. Additionally, all the emulsions containing CNF also manifested resistance against interfacial disruption caused by gravity, collision and other effects during long-term storage. The hydrophilic CNFs with abundant hydroxyl groups have the tendency to overlap and join together into entangled networks and form macroscopic gels, acting as viscosity modifiers and thickeners in aqueous media at relatively low concentrations. The formation of this very high viscosity and gel-like behavior medium may trap the continuous phase between the droplets inside the network, thereby inhibiting gravity-induced creaming and serum separation during extended emulsion storage. Furthermore, the avocado oil/water emulsions formulated with 1% CNFs were able to remain its integrity after storage for 30 days, in tandem with heat treatment up to 80 °C and at extreme acidic (pH 2) or alkaline (pH 11) conditions (Szlapak Franco et al., 2020). The findings suggested that CNFs isolated from peach palm residues might be a propitious replacement for conventional surfactant (e.g., sorbitan monostearate) to deliver an edible emulsion with superior stability.

4.2   Biomedical Field

Nanocellulose is also commonly used in biomedical applications due to its superb mechanical properties, large specific surface area, availability for versatile surface functionalization, non-toxicity and biocompatibility (Mishra et al., 2018; Shazali et al., 2019). Nanocellulose membrane had captivated increased research interest for cell attachment and proliferation due to its unique 3D network, excessive porosity and low cytotoxicity. In this regard, the cell attachment can be enhanced via surface functionalization of nanocellulose such as the introduction of surface charges, plasma treatment method or protein coatings. Withal, the substantial water-holding capability, excellent flexibility and durability of nanocellulose membrane also rendered it

a propitious material for wound dressing. Over the past decade, nanocellulose structured drug delivery systems have been adapted to regulate the drug release rates and subsequent drug levels in the bloodstream. One prominent example is the usage of nanocellulose-based hydrogel as a carrier for various kinds of drugs delivery (Mishra et al., 2018). The detailed summary of the most well-known nanocellulose hydrogel processing methods and their latest advanced applications are available in the work of Padzil's group (Padzil et al., 2020).

The short circulatory half-life and poor bioavailability of water-insoluble drug (e.g., anticancer drugs) have always been the major hurdles for efficient drug delivery inside the human body. Generally, rod-shaped particles can be regarded as a good drug carrier owing to its high cellular uptake in the body, long circulatory time and tumour accumulation. For instance, CNCs with rod-liked structure demonstrate great potential for drug delivery due to its high surface area and abundance of surface hydroxyl groups that allow its surface functionalization, thus facilitating a high level of drug loading. Recently, Foo and co-workers successfully attached curcumin onto CNC derived from EFB modified with tannic acid (TA) and decylamine (DA) as a superior and sustainable drug carrier (Foo et al., 2019). The modified CNC could replace the conventional surfactant, cetyl trimethylammonium bromide which might interact with the phospholipid bilayers of cells and lead to cell death. Curcumin is used because it possesses outstanding anti-inflammatory, antioxidant, antimicrobial, anticancer and antimutagenic properties. The authors reported that the curcumin binding capacity of surface-modified CNC was two-fold higher than pristine CNC, regardless of the concentration of curcumin used. This can be attributed to the increased hydrophobicity level of modified CNC that favored the hydrophobic interaction between the phenolic moieties of curcumin and long alkyl chain of DA, therefore yielding the remarkable curcumin binding efficiency ranging from 95 to 99%. Moreover, the formation of entangled and crosslinked network might also facilitate the binding of curcumin particles onto the surface of modified CNC. The schematics illustrating possible mechanisms for binding of curcumin onto surface of CNC modified with TA and DA are given in Fig. 4a (Foo et al., 2019). This work has proven that the surface modification using both TA and DA is a feasible approach to tailor the properties of CNC as an effective drug carrier.

In another similar study, Shazali and associates synthesized spherical CNC from EFB conjugated with fluorescein isothiocyanate (FITC) and investigated its cellular internalization into C6 (rat glioma) and NIH3T3 (normal murine fibroblast) cells for potential anticancer drug nanocarrier application (Shazali et al., 2019). Interestingly, the FITC-CNC showed poor cellular uptake into both normal and cancerous cell lines. Theoretically, the C6 and NIH3T3 take up nanoparticles via non-specific adsorptive endocytosis, which was governed by the surface charge, shape and hydrophobicity of the particles. Howbeit, the cellular accumulation in this study was inhibited due to the electrostatic repulsion between both negatively charged CNC surface and the cell membrane of fibroblasts (Fig. 4b). Consequently, the CNC failed to adhere to the cell surface in order to initiate membrane wrapping (Shazali et al., 2019). Therefore, FITC-CNC can be developed into targeted nanocarrier for the delivery of anticancer drugs by tuning its surface charge properties to enhance its cellular uptake
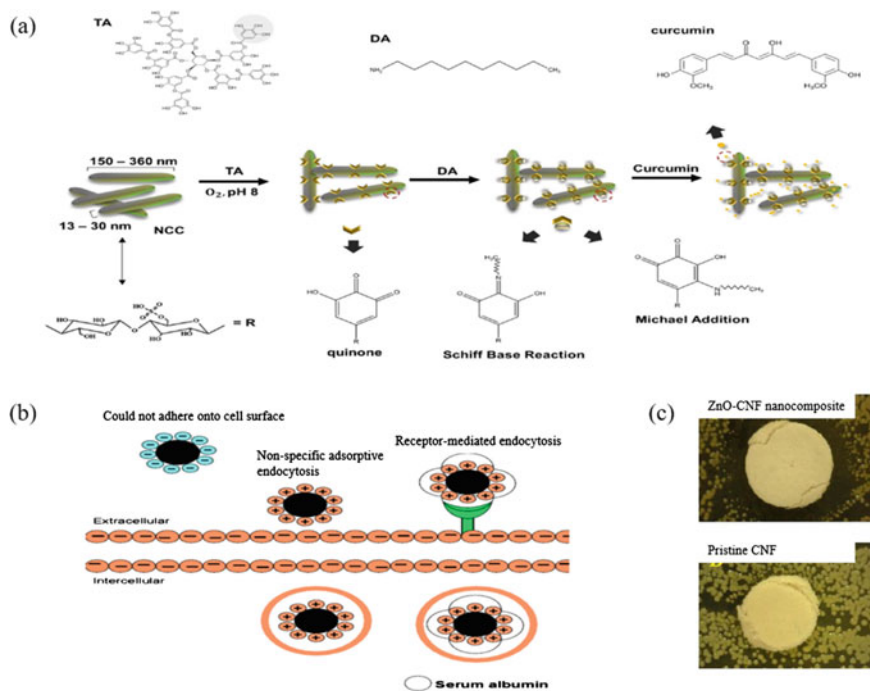
Fig. 4 **a** Schematic illustration of possible mechanism for binding of curcumin onto CNC surface modified with tannic acid (TA) and decylamine (DA), **b** illustration of possible uptake mechanism of FITC-CNC nanospheres with different surface charges and **c** enlarged image of ZnO-CNF and pristine CNF nanocomposite film in antibacterial test (Foo et al., 2019; Shazali et al., 2019; Supramaniam et al., 2020)

into cancerous cells. Furthermore, Supramaniam and colleagues fabricated oil palm biomass-derived CNFs loaded with zinc oxide (ZnO) nanocomposites for wound care application (Supramaniam et al., 2020). The wound disease caused by bacteria such as Methicillin-resistant *Staphylococcus aureus* (MRSA) can delay wound healing and leads to exudate development on the injured surface. ZnO has received considerable attention in nanofiller-related research due to its antibacterial activity, good photocatalytic performance, non-toxicity and high stability. They discovered that the ZnO-CNFs possessed higher swelling capacity (10%) compared to pristine CNF. This can be ascribed to the presence of interstitial pores in cellulosic polymeric network and charged ZnO nanoparticles that result in the seepage of water molecules to balance the increase of ion osmotic pressure. Based on Fig. 4c, the ZnO-CNF sample also exhibited 2 mm inhibition zone for MRSA antibacterial test, while no inhibition zone was observed for pristine CNF. The antibacterial property of ZnO might be attributed to the generation of reactive oxygen species (ROS) such as superoxide radicals, hydroxyl radicals and singlet oxygen. These ROS can then induce oxidative stress and interrupt the transmembrane electron transport, which will damage

the DNA structure and ultimately lead to cell death (Supramaniam et al., 2020). The results from this study suggested that the as-prepared ZnO-CNF nanocomposites can be utilized as potential nanofillers for wound dressing application.

4.3 Effluent Treatment

The rapid development of petrochemical industries and urbanization is responsible for the massive deterioration in water quality due to the contamination from heavy metals and hazardous or toxic chemicals. These contaminants pose a severe threat to human health and ecological well-being (Septevani et al., 2020; Shanmugarajah et al., 2019). Hitherto, many techniques have been developed for both organic and heavy metal water remediation including electrochemical, physicochemical treatment, membrane filtration, photocatalysis, biological treatment and adsorption. Among all these methods, adsorption is the most promising and cost-effective technique due to its high efficiency, scalable processability and ease of operation (Septevani et al., 2020). Specifically, cellulose-based adsorbents have garnered interest for water remediation because of its hydrophilicity, high specific surface area, ease of chemical surface modification, non-toxicity, high adsorption affinity toward many classes of pollutants and 100% biodegradable with no adverse effect on the environment and human beings (Septevani et al., 2020; Thomas et al., 2018).

Some of the common organic contaminants in drinking water are natural oils, dyes, chemical pesticides and synthetic medicines materials (Mishra et al., 2018). For instance, methylene blue (MB) is a cationic dye that is commonly employed in the textile dyeing industry. It is poisonous since acute exposure could cause nausea, increased heartbeat and breathing difficulties. Recently, Shanmugarajah and co-workers managed to convert EFB into CNCs without further surface modification as a promising natural bio-sorbent for the removal of MB (Shanmugarajah et al., 2019). They found that the percentage of MB removal increased rapidly from 60 to 87% with increase of CNC dosage from 0.005 to 0.01 g, but the removal rate remained constant when the CNC dosage increased further from 0.01 to 0.05 g. Higher dose of CNC will increase the active sites available on the adsorbents to bind with more dye molecules, implying a quick initial adsorption with better removal efficiency. However, further increase in adsorbent dosage will cause particle aggregation and subsequently reduce the efficiency for dye removal. Withal, the optimal adsorption occurred in alkaline medium (pH 8) with removal rate of 88%. This is because the presence of OH^- ions in the dye solution would create better electrostatic attractions for more dye molecular binding, which is particularly important for cationic dyes such as MB. On the other hand, the adsorption rate at strong acidic condition (pH 2) was only 29% due to the excess H^+ ions competing with the cationic dye for adsorption sites on CNC surface (Fig. 5a). The negatively charged sulfate ions on the surface of CNCs were also protonated under acidic condition, hence reducing the binding efficiency with MB molecules. The authors also reported good adsorption capacity (50.91 mg/g) at very low pristine CNC dosage of 0.066 mg/ml attributed to the
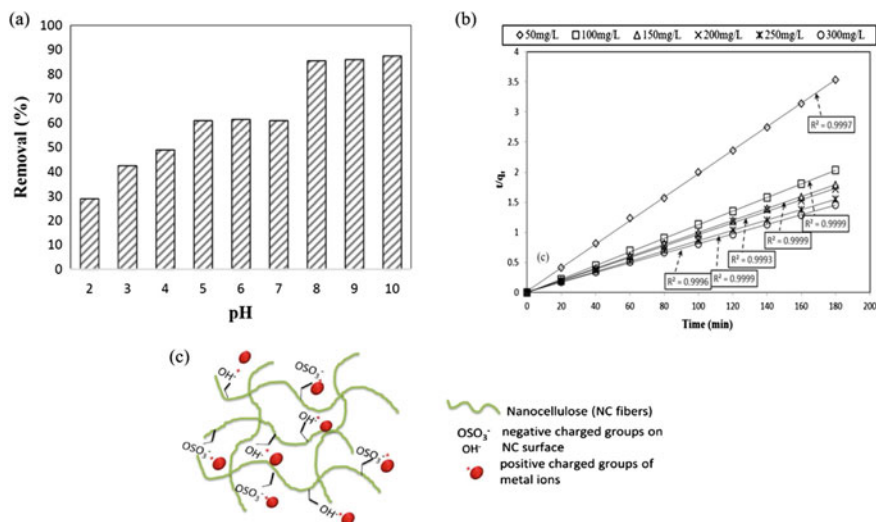
Fig. 5 **a** Removal of methylene blue by CNCs at different pH values, **b** pseudo-second order kinetic model for adsorption of methylene blue at various initial dye concentrations and **c** schematic of electrostatic interaction on the surface of nanocellulose bio-adsorbents (Septevani et al., 2020; Shanmugarajah et al., 2019)

abundant and highly functional methylol and hydroxyl groups on the nanocellulose. Figure 5b illustrates that the adsorption obeyed Langmuir isotherm and pseudo-second order kinetic model with the estimated maximum adsorption capacity of 144.93 mg/g, where chemisorption was the rate-controlling factor (Shanmugarajah et al., 2019).

In another similar study conducted by Septevani's group, EFB-based nanocellulose functionalized with activated carbon (AC) was successfully fabricated as a super-adsorbent for water remediation (Septevani et al., 2020). Surprisingly, the functionalization of AC on nanocellulose did not improve the metal adsorption, therefore confirming that the micron size AC will disrupt the network structure of nanocellulose and reduce the active adsorption sites, which yielded a lower heavy metal performance. The optimum dose for heavy metals removal is 2% of nanocellulose extracted via sulfuric acid hydrolysis (NCS) with removal efficiencies of 80%, 9% and 8% for Pb^{2+}, Cd^{2+} and Cr^{3+}, respectively (Septevani et al., 2020). The adsorption capacity toward Pb^{2+} is substantially higher than other metal ions due to the lower hydration energy of Pb^{2+}, which increased the ion interaction toward the activated sites of super-adsorbent. Additionally, the formation of sulfate groups on the surface of NCS during acid hydrolysis may enhance the heavy metal adsorption capacity since the sulfonated nanocellulose possess a large number of binding sites for the electrostatic interaction between the negatively charged sulfate groups and the positively charged metal ions (Fig. 5c). The authors also reported that the optimum adsorption efficiency for 2% NCS was 80% at initial metal ion concentration of
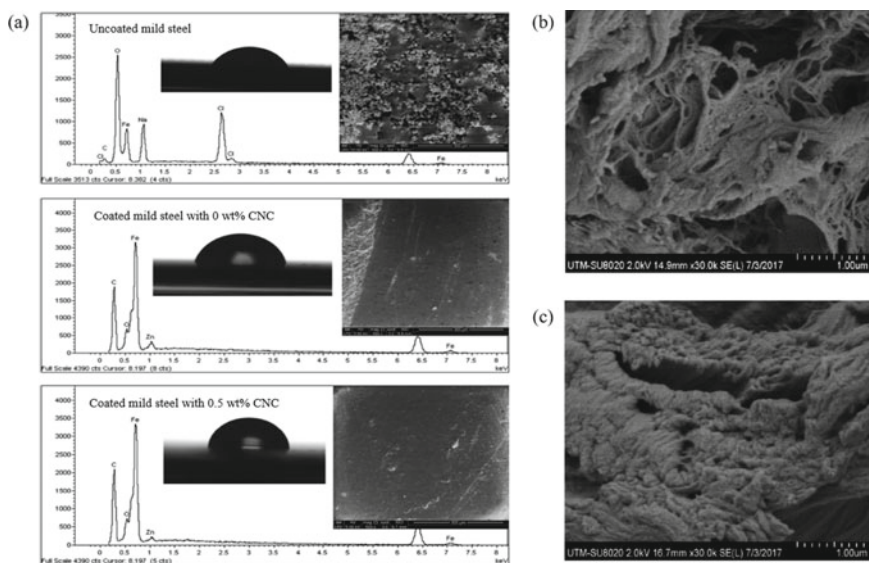
Fig. 6 **a** EDX spectra (×500 magnification), SEM image (×500 magnification and 300 μm scale) and water contact angle for mild steel reinforced epoxy-Zn rich coating with CNC, FESEM image of **b** lyophilized chitosan/nanocellulose and **c** lyophilized CRL/chitosan-nanocellulose biocatalysts (Azani et al., 2020; Elias et al., 2017)

30 ppm (Septevani et al., 2020). Increasing the initial metal ion concentration will accelerate the diffusion of metal ion onto the adsorbent until all the active sites on the nanocellulose adsorbent attain the saturation point. Once the saturation point was reached, the adsorption capacity remained constant while the adsorption efficiency gradually reduced. Furthermore, the optimum adsorption time was reported at 150 s, where the maximum adsorption efficiency and adsorption capacity for Pb^{2+} were 86% and 30.45 mg/g, respectively. The adsorption process obeyed the Langmuir isotherm model, where the adsorption occurred on the surface of solid following the monolayer sorption mechanism, which is consistent with the findings of Shanmugarajah and associates (Septevani et al., 2020; Shanmugarajah et al., 2019). The lead adsorption capacity reduced to 10.34 mg/g and 7.80 mg/g after the second and third cycles of nanocellulose adsorbent regeneration, respectively (Septevani et al., 2020). The significant decline of adsorption capacity might be due to the fact that the super-adsorbent was derived from easily degradable biomass sources such as EFB. The authors also examined the effect of nanocellulose super-adsorbent on the organic pollutant remediation and recorded the highest chemical oxygen demand removal of 93% after treatment with 0.5 wt% sulfonated nanocellulose functionalized with AC. Forbye, the treated water quality remained within the government specifications with pH and TDS level of 7.5 and 151 mg/L, respectively (Septevani et al., 2020). This indicated that nanocellulose derived from oil palm biomass can be utilized as robust and effective adsorbents for effluent treatment.

4.4   Miscellaneous

In addition to the food industry, biomedical field and effluent treatment, a recent shift toward the utilization of nanocellulose in building materials, corrosion protection and biocatalyst was observed in the research community. In particular, Mocktar and colleagues incorporated oil palm nanocellulose that acts as nanofillers into composite bricks to reduce the radon gas emanations in the indoor environment (Mocktar et al., 2020). Radon gas is notorious for causing lung cancer besides smoking. It is noteworthy that brick material is one of the significant sources of indoor radon emanations, in which the aggregates contain Ra-226 that will decay to Rn-222 and alpha particles. These alpha particles with high linear energy transfer property can eventually damage the DNA double bonding in humans, where it will be lodged in the lining of the lungs and release mass radiation energies. Nanocellulose can be incorporated into building materials to minimize the indoor radon concentration since the cellulosic materials will act as liquid fillers to substitute the radon sources such as gravel, cement and sand. The authors discovered that the radon concentration for composite bricks with 40 mL and 80 mL nanocellulose was 1.4 and 2.17 pCi per 1, respectively. Howbeit, further increase of nanocellulose contents (120 mL, 160 mL, 200 mL) led to higher radon concentration because more water was used to fabricate the bricks, thus resulting in the swelling of cellulose chain and increased moisture uptake. The high humidity environment will in turn increase the radon concentration due to the interactions of alpha particles with water molecules. The fibrillar networks of nanocellulose will also miniaturize the porosity of the composite bricks and reduce the formation of cracks, which indirectly help to mitigate the radon gas emission. The difference in radon concentrations between the control and composite bricks with 40 mL nanocellulose were 2.84 pCi per 1 and this could increase the probability of lung cancer. This is because for every 2.7 pCi per 1 radon exposure, the probability of lung cancer will be raised for approximately 16% in an indoor environment. In addition, the composite brick reinforced with 40 mL nanocellulose exhibited higher Young's modulus (27.8 MPa) compared to the control brick (27 MPa), indicating the high stiffness of composite brick materials (Mocktar et al., 2020). The results proved that this type of novel building materials can promote a healthy environment and contribute toward a better life.

Corrosion has become one of the biggest concerns in the marine, oil and gas, automotive and construction industries. Hence, corrosion protection is essential to ensure the production of high-quality products with relatively lower maintenance cost. The high toxicity of conventional chromate-based coating to the environment have urged researchers to develop state-of-the-art anticorrosive organic coating with high performance. In general, the epoxy-Zn rich coating has been widely used to protect the steel substrate in various industries. This is because the electrical contact of zinc particle in epoxy coating system offers excellent protection to the metal substrate against corrosive agents and ions such as H_2O_2, O_2 and Cl_2. The high crosslinking density of epoxy coating also provides good adhesion to the metal surface. Nevertheless, the epoxy coating might experience considerable mechanical

damage when exposed to aggressive environment for an extended period of time. One possible solution is to introduce nanocellulose-based composites to enhance its adhesion to metal surface and durability in order to minimize the metal corrosions. For instance, Azani and associates successfully reinforced epoxy-Zn rich coating with CNCs derived from OPF to improve the corrosion protection of mild steel (Azani et al., 2020). Based on the results obtained from corrosion studies, the mild steel coated with epoxy-Zn rich at 0.5 wt% CNC was the optimum loading since it lessened the corrosion by 99%, exhibited highest hydrophobicity with water contact angle of $100.5 \pm 0.7°$ and a meagre amount of O element on the coating surface, indicating a low corrosion rate (Fig. 6a). The high surface area of CNCs ($26.10 \, m^2/g$) can simulate the growth of crosslinking within the epoxy coating network and the compact size of CNCs with diameter less than 100 nm can easily penetrate the coating surface, thus eliminating any damage or crack to prevent the penetration of any corrosive species into the metal surface. Nonetheless, when large amount of nanocellulose was added, the formation of strong hydrogen bonds between the nanocrystals might cause aggregation of epoxy coating. This might deteriorate the anticorrosion performance of coating due to the formation of small pores within the epoxy network, which will allow the contact of corrosive species with the metal surface (Azani et al., 2020). Therefore, small amount of CNCs (<1 wt%) was sufficient to ameliorate the mechanical strength and performance of epoxy coating in minimizing corrosion.

Furthermore, Elias's group utilized nanocellulose isolated from OPF leaves/chitosan nanocomposite as support material for immobilizing *Candida rugosa lipase* (CRL) to catalyze the production of butyl butyrate through esterification of butanol and butyric acid (Elias et al., 2017). Both nanocellulose and chitosan were chosen due to their biocompatibility, good mechanical strength, non-toxicity, amenability for chemical modification and environmentally friendliness. CRL as free lipases are known to be easily deactivated under harsh industrial processing conditions, thereby limiting their use in catalyzing chemical processes such as esterification, transesterification and interesterification. Hence, immobilizing CRL onto nanocellulose/chitosan hybrid composites might enhance the operational stability of the enzyme and improve its catalytic performance in aqueous and non-aqueous conditions, as well as enabling catalyst recovery and reuse for large-scale applications. The authors reported that the air-dried chitosan-nanocellulose support showed higher immobilized protein of 5.20 mg/g compared to 4.80 mg/g in the lyophilized chitosan-nanocellulose. This is because higher numbers of internally located pores were formed during lyophilization compared to the pores that are exposed to the outer environment (Fig. 6b). In other words, there were fewer surface cavities available on chitosan-nanocellulose support for the attachment of CRL and also lesser CRL with its active sites exposed to the surface for catalysis reaction (Fig. 6c). Therefore, 73.8% conversion of butyl butyrate was reported for CRL immobilized on air-dried chitosan-nanocellulose in 3 h, while only a mere 25% conversion of the ester was observed for CRL immobilized on lyophilized chitosan-nanocellulose. Moreover, the as-synthesized CRL/chitosan-nanocellulose yielded 76.3% of butyl butyrate within only 4 h. Longer immobilization durations beyond 4 h were futile and produced significantly fewer active batches of CRL/chitosan-nanocellulose biocatalysts.

This is because optimal immobilization duration is indispensable to allow formation of covalent bonds between the CRL and chitosan-nanocellulose support (Elias et al., 2017). This work had demonstrated the feasibility of using the highly functional CRL/chitosan-nanocellulose biocatalysts prepared from OPF leaves biomass to produce high yields of butyl butyrate.

5 Conclusion and Future Recommendations

The generation of enormous amounts of oil palm biomass in Malaysia caused a plethora of environmental issues despite the contribution of palm oil industry to the country's growth and development. The concept of waste valorization of oil palm biomass is an innovative idea that can bring imponderable economic and ecological benefits. The utilization of nanotechnology to produce nanocellulose from oil palm biomass has broad application prospects compared with the conventional disposal methods such as incineration and composting. Nanocellulose is abundant, non-toxic, renewable, biodegradable and has excellent mechanical properties, rendering it a highly propitious candidate to play a key role in the synthesis of many state-of-the-art nanocomposite materials. Nanocellulose has been scrutinized not only for its applications in food packaging films and emulsions, but also in much more surprising domains such as drug carriers, wound dressing, bio-sorbents for water remediation, building materials, corrosion protection and biocatalysts. However, there are several challenges that need to be addressed by the academia and industrial experts before the official roll-out of nanocellulose-based materials into the society. First, life cycle assessment must be conducted to identify and analyze the potential risk circumstances of nanocellulose-based composites. This is to ensure that nanocellulose does not pose any harm toward human health and the environment. Specifically, life cycle assessment should include detailed analysis during the extraction of raw materials, production, transportation, consumption and final disposal. In addition, the advanced 3D simulation software endorsed by machine learning and Industrial Revolution 4.0, coupled with atomistic and analytical modelling shall be utilized to further understand the structure-property relationship of the novel nanocellulose-based materials (e.g., packaging films, membranes or catalysts). This will provide an adequate guideline for the synthesis and design of nanocellulose composite products with desired properties or characteristics. The incorporation of artificial intelligence, Internet of Things and big data analytics presents an auspicious approach to achieve the fully automated manufacturing process of advanced nanocellulose-containing materials without human intervention in the coming years (Lim et al., 2022). Consequently, it represents a cornerstone in realizing the sustainable consumption and production patterns that aligned with the United Nations' Sustainable Development Goals.

References

Adel, A. M., Ibrahim, A. A., El-Shafei, A. M., & Al-Shemy, M. T. (2019). Inclusion complex of clove oil with chitosan/β-cyclodextrin citrate/oxidized nanocellulose biocomposite for active food packaging. *Food Packaging and Shelf Life, 20*, 100307.

Aditiawati, P., Dungani, R., & Amelia, C. (2018). Enzymatic production of cellulose nanofibers from oil palm empty fruit bunch (EFB) with crude cellulase of *Trichoderma* sp. *Materials Research Express, 5*(3), 034005. https://doi.org/10.1088/2053-1591/aab449

Alonso, D. M., Wettstein, S. G., & Dumesic, J. A. (2012). Bimetallic catalysts for upgrading of biomass to fuels and chemicals. *Chemical Society Reviews, 41*(24), 8075–8098.

Azani, N. F. S. M., Haafiz, M. K. M., Zahari, A., Poinsignon, S., Brosse, N., & Hussin, M. H. (2020). Preparation and characterizations of oil palm fronds cellulose nanocrystal (OPF-CNC) as reinforcing filler in epoxy-Zn rich coating for mild steel corrosion protection. *International Journal of Biological Macromolecules, 153*, 385–398. https://doi.org/10.1016/j.ijbiomac.2020.03.020

Azeredo, H. M., Rosa, M. F., & Mattoso, L. H. C. (2017). *Nanocellulose in Bio-Based Food Packaging Applications., 97*, 664–671.

Bhardwaj, A., Alam, T., Sharma, V., Alam, M. S., Hamid, H., & Deshwal, G. K. (2020). Lignocellulosic agricultural biomass as a biodegradable and eco-friendly alternative for polymer-based food packaging. *Journal of Packaging Technology and Research*, 1–12.

Bharimalla, A., Deshmukh, S., Vigneshwaran, N., Patil, P., & Prasad, V. (2017). Nanocellulose-polymer composites for applications in food packaging: Current status, future prospects and challenges. *Polymer-Plastics Technology and Engineering, 56*(8), 805–823.

Campos et al., 2017 Campos, A. D., Neto, A. R. D. S., Rodrigues, V. B., Kuana, V. A., Correa, A. C., Takahashi, M. C., Mattoso, L. H., & Marconcini, J. M. (2017). Production of Cellulose nanowhiskers from oil palm mesocarp fibers by acid hydrolysis and microfluidization. *Journal of Nanoscience and Nanotechnology, 17*(7), 4970–4976. https://doi.org/10.1166/jnn.2017.13451

Dai, H., Ou, S., Huang, Y., & Huang, H. (2018). Utilization of pineapple peel for production of nanocellulose and film application. *Cellulose, 25*(3), 1743–1756.

El Miri, N., Abdelouahdi, K., Barakat, A., Zahouily, M., Fihri, A., Solhy, A., & El Achaby, M. (2015). Bio-nanocomposite films reinforced with cellulose nanocrystals: Rheology of film-forming solutions, transparency, water vapor barrier and tensile properties of films. *Carbohydrate Polymers, 129*, 156–167. https://doi.org/10.1016/j.carbpol.2015.04.051

Elias, N., Chandren, S., Attan, N., Mahat, N. A., Razak, F. I. A., Jamalis, J., & Wahab, R. A. (2017). Structure and properties of oil palm-based nanocellulose reinforced chitosan nanocomposite for efficient synthesis of butyl butyrate. *Carbohydrate Polymers, 176*, 281–292. https://doi.org/10.1016/j.carbpol.2017.08.097

Fang, Z., Hou, G., Chen, C., & Hu, L. (2019). Nanocellulose-based films and their emerging applications. *Current Opinion in Solid State and Materials Science, 23*(4), 100764. https://doi.org/10.1016/j.cossms.2019.07.003

Foo, M. L., Tan, C. R., Lim, P. D., Ooi, C. W., Tan, K. W., & Chew, I. M. L. (2019). Surface-modified nanocrystalline cellulose from oil palm empty fruit bunch for effective binding of curcumin. *International Journal of Biological Macromolecules, 138*, 1064–1071. https://doi.org/10.1016/j.ijbiomac.2019.07.035

Gan, P. G., Sam, S. T., Abdullah, M. F., Omar, M. F., & Tan, L. S. (2020). An alkaline deep eutectic solvent based on potassium carbonate and glycerol as pretreatment for the isolation of cellulose nanocrystals from empty fruit bunch. *BioResources, 15*(1), 1154–1170.

Gea, S., Siregar, A. H., Zaidar, E., Harahap, M., Indrawan, D. P., & Perangin-Angin, Y. A. (2020). Isolation and Characterisation of Cellulose Nanofibre and Lignin from Oil Palm Empty Fruit Bunches. *Materials, 13*(10). https://doi.org/10.3390/ma13102290

Guzman-Puyol, S., Ceseracciu, L., Tedeschi, G., Marras, S., Scarpellini, A., Benítez, J. J., Athanassiou, A., & Heredia-Guerrero, J. A. (2019). Transparent and robust all-cellulose nanocomposite

packaging materials prepared in a mixture of trifluoroacetic acid and trifluoroacetic anhydride. *Nanomaterials, 9*(3), 368. https://doi.org/10.3390/nano9030368

Huang, L., Zhao, H., Yi, T., Qi, M., Xu, H., Mo, Q., Huang, C., Wang, S., & Liu, Y. (2020). Preparation and properties of cassava residue cellulose nanofibril/cassava starch composite films. *Nanomaterials, 10*(4), 755.

Jiang, J., Zhu, Y., & Jiang, F. (2021). Sustainable isolation of nanocellulose from cellulose and lignocellulosic feedstocks: Recent progress and perspectives. *Carbohydrate Polymers*, 118188.

Lamaming, J., Hashim, R., Leh, C. P., Sulaiman, O., & Lamaming, S. Z. (2020). Bio-nanocomposite films reinforced with various types of cellulose nanocrystals isolated from oil palm biomass waste. *Waste and Biomass Valorization, 11*(12), 7017–7027. https://doi.org/10.1007/s12649-019-008 92-7

Lim, H. J., Cheng, W. K., Tan, K. W., & Yu, L. J. (2022). Oil palm-based nanocellulose for a sustainable future: Where are we now? *Journal of Environmental Chemical Engineering, 10*(2), 107271. https://doi.org/10.1016/j.jece.2022.107271

Ma, T., Hu, X., Lu, S., Liao, X., Song, Y., & Hu, X. (2020). Nanocellulose: a promising green treasure from food wastes to available food materials. *Critical Reviews in Food Science and Nutrition*, 1–14. https://doi.org/10.1080/10408398.2020.1832440

Malucelli, L. C., Lacerda, L. G., Dziedzic, M., & da Silva Carvalho Filho, M. A. (2017). Preparation, properties and future perspectives of nanocrystals from agro-industrial residues: A review of recent research. *Reviews in Environmental Science and Bio/technology, 16*(1), 131–145. https://doi.org/10.1007/s11157-017-9423-4

Mazlita, Y., Lee, H. V., & Hamid, S. B. A. (2016). preparation of cellulose nanocrystals bio-polymer from agro-industrial wastes: Separation and characterization. *Polymers and Polymer Composites, 24*(9), 719–728. https://doi.org/10.1177/096739111602400907

Mishra, R. K., Sabu, A., & Tiwari, S. K. (2018). Materials chemistry and the futurist eco-friendly applications of nanocellulose: Status and prospect. *Journal of Saudi Chemical Society, 22*(8), 949–978. https://doi.org/10.1016/j.jscs.2018.02.005

Mocktar, F. A., Abdul razab, M. K. A., & Mohamed noor, A. A. (2020). Incorporating kenaf and oil palm nanocellulose in building materials for indoor radon gas emanation reduction. *Radiation Protection Dosimetry, 189*(1), 69–75. https://doi.org/10.1093/rpd/ncaa014 %J

Mohamed, M. A., Salleh, W. N. W., Jaafar, J., Asri, S. E. A. M., & Ismail, A. F. (2015). Physicochemical properties of "green" nanocrystalline cellulose isolated from recycled newspaper. *Rsc Advances, 5*(38), 29842–29849. https://doi.org/10.1039/C4RA17020B

Onoja, E., Chandren, S., Abdul Razak, F. I., Mahat, N. A., & Wahab, R. A. (2019). Oil palm (*Elaeis guineensis*) biomass in Malaysia: The present and future prospects. *Waste and Biomass Valorization, 10*(8), 2099–2117. https://doi.org/10.1007/s12649-018-0258-1

Padzil, F. N., Lee, S. H., Ainun, Z. M., Lee, C. H., & Abdullah, L. C. (2020). Potential of oil palm empty fruit bunch resources in nanocellulose hydrogel production for versatile applications: A review. *Materials, 13*(5). https://doi.org/10.3390/ma13051245

Parveez, G. K. A., Tarmizi, A. H. A., Sundram, S., Loh, S. K., Ong-Abdullah, M., Palam, K. D. P., Salleh, K. M., Idris, Z. (2021). Oil palm economic performance in Malaysia and R&D progress in 2020. *Journal of Oil Palm Research, 33*, 2.

Perrin, L., Gillet, G., Gressin, L., & Desobry, S. (2020). Interest of pickering emulsions for sustainable micro/nanocellulose in food and cosmetic applications. *Polymers, 12*(10). https://doi.org/10.3390/polym12102385

Rubinsin, N. J., Daud, W. R. W., Kamarudin, S. K., Masdar, M. S., Rosli, M. I., Samsatli, S., Tapia, J. F. D., Ghani, W. A. W. A. K., Hasan, A., & Lim, K. L. (2021). Modelling and optimisation of oil palm biomass value chains and the environment–food–energy–water nexus in peninsular Malaysia. *Biomass and Bioenergy, 144*, 105912.

Salehudin, M. H., Salleh, E., Muhamad, I. I., & Mamat, S. N. H. (2014). Starch-based biofilm reinforced with empty fruit bunch cellulose nanofibre. *Materials Research Innovations, 18*(sup6), S6-322–S326-325. https://doi.org/10.1179/1432891714Z.000000000977

Septevani, A. A., Rifathin, A., Sari, A. A., Sampora, Y., Ariani, G. N., Sudiyarmanto, & Sondari, D. (2020). Oil palm empty fruit bunch-based nanocellulose as a super-adsorbent for water remediation. *Carbohydrate Polymers, 229*, 115433. https://doi.org/10.1016/j.carbpol.2019.115433

Shanmugarajah, B., Chew, I. M., Mubarak, N. M., Choong, T. S., Yoo, C., & Tan, K. (2019). Valorization of palm oil agro-waste into cellulose biosorbents for highly effective textile effluent remediation. *Journal of Cleaner Production, 210*, 697–709. https://doi.org/10.1016/j.jclepro.2018.10.342

Shazali, N. A., Zaidi, N. E., Ariffin, H., Abdullah, L. C., Ghaemi, F., Abdullah, J. M., Takashima, I., & Nik Abd. Rahman, N. M. (2019). Characterization and cellular internalization of spherical cellulose nanocrystals (CNC) into normal and cancerous fibroblasts. *Materials, 12*(19). https://doi.org/10.3390/ma12193251

Sinaga, M. Z. E., Gea, S., Panindia, N., & Sihombing, Y. A. (2018). The preparation of all-cellulose nanocomposite film from isolated cellulose of corncobs as food packaging. *Oriental Journal of Chemistry, 34*(1), 562.

Solikhin, A., Hadi, Y. S., Massijaya, M. Y., & Nikmatin, S. (2017). Novel isolation of empty fruit bunch lignocellulose nanofibers using different vibration milling times-assisted multimechanical stages. *Waste and Biomass Valorization, 8*(7), 2451–2462. https://doi.org/10.1007/s12649-016-9765-0

Solikhin, A., Hadi, Y. S., Massijaya, M. Y., Nikmatin, S., Suzuki, S., Kojima, Y., & Kobori, H. (2018). Properties of poly(vinyl alcohol)/chitosan nanocomposite films reinforced with oil palm empty fruit bunch amorphous lignocellulose nanofibers. *Journal of Polymers and the Environment, 26*(8), 3316–3333. https://doi.org/10.1007/s10924-018-1215-6

Supian, M. A. F., Amin, K. N. M., Jamari, S. S., & Mohamad, S. (2020). Production of cellulose nanofiber (CNF) from empty fruit bunch (EFB) via mechanical method. *Journal of Environmental Chemical Engineering, 8*(1), 103024. https://doi.org/10.1016/j.jece.2019.103024

Supramaniam, J., Kiat Wong, S., Fen Leo, B., Teng Hern Tan, L., Hing Goh, B., & Ying Tang, S. (2020). Unravelling the swelling behaviour and antibacterial activity of palm cellulose nanofiber-based metallic nanocomposites. *IOP Conference Series: Materials Science and Engineering, 778*, 012027. https://doi.org/10.1088/1757-899x/778/1/012027

Szlapak Franco, T., Martínez Rodríguez, D. C., Jiménez Soto, M. F., Jiménez Amezcua, R. M., Urquíza, M. R., Mendizábal Mijares, E., & de Muniz, G. I. B. (2020). Production and technological characteristics of avocado oil emulsions stabilized with cellulose nanofibrils isolated from agroindustrial residues. *Colloids and Surfaces A: Physicochemical and Engineering Aspects, 586*, 124263. https://doi.org/10.1016/j.colsurfa.2019.124263

Tan, K., Heo, S., Foo, M., Chew, I. M., & Yoo, C. (2019). An insight into nanocellulose as soft condensed matter: Challenge and future prospective toward environmental sustainability. *Science of the Total Environment, 650*, 1309–1326. https://doi.org/10.1016/j.scitotenv.2018.08.402

Tang, Y., Zhang, X., Zhao, R., Guo, D., & Zhang, J. (2018). Preparation and properties of chitosan/guar gum/nanocrystalline cellulose nanocomposite films. *Carbohydrate Polymers, 197*, 128–136. https://doi.org/10.1016/j.carbpol.2018.05.073

Thomas, B., Raj, M. C., B, A. K., H, R. M., Joy, J., Moores, A., Drisko, G.L., & Sanchez, C. (2018). nanocellulose, a versatile green platform: From biosources to materials and their applications. *Chemical Reviews, 118*(24), 11575–11625. https://doi.org/10.1021/acs.chemrev.7b00627

Vilarinho, F., Sanches Silva, A., Vaz, M. F., & Farinha, J. P. (2018). Nanocellulose in green food packaging. *Critical Reviews in Food Science and Nutrition, 58*(9), 1526–1537.

Yahya, M. B., Lee, H. V., & Abd Hamid, S. B. (2015). Preparation of nanocellulose via transition metal salt-catalyzed hydrolysis pathway. *BioResources, 10*(4), 7627–7639.